Arch. Metall. Mater. **67** (2022), 2, 479-485

DOI: https://doi.org/10.24425/amm.2022.137780

M. LUȚCANU[1,3], M. COTEAȚĂ[2], M.A. BERNEVIG[1], C.D. NECHIFOR[3], M.M. CAZACU[3], P. PARASCHIV[4], B. ISTRATE[5], G. BĂDĂRĂU[1], I.G. SANDU[1], N. CIMPOEȘU[1*]

OBTAINING AND ANALYZING THE Al_2O_3-ZrO_2 CERAMIC LAYERS ON METALLIC SUBSTRATE

In this case ceramic layers from Metco ZrO_2 and Al_2O_3 powders mixture (25/75; 50/50 and 75/25) were obtained through atmospheric plasma spraying (APS) after five passes on low carbon steel substrate. The sample surfaces mechanically grinded (160-2400) before and after ceramic layer deposition. Powder's mixtures and the surface of ceramic thin layers were analyzed through: scanning electron microscopy (SEM). In order to understand the effect of surface wettability of the ceramic layers, before and after grinding the surface, three different liquids were used. Experimental results confirm the modification of the steel substrate surface characteristic from hydrophilic to hydrophobic when the ceramic layer was deposited. Surface free energy of hydration increases for all the samples with zirconia percentage addition before polishing process.

Keywords: ceramic layer; atmospheric plasma spraying; SEM; EDS

1. Introduction

Ceramic layers present an increasing interest in many industrial and medical applications based on their excellent properties of high hardness, corrosion (electro-corrosion) and temperature resistance [1]. Ceramic materials have, especially, in last year's more and more applications in different fields as bulk and also as ceramic layers (thin and very thin) [2,3]. Between ceramic materials those oxides like zirconia and alumina present a special attraction based on their properties. Different methods were used to grow ceramic layers based on Al_2O_3 and ZrO_2 like chemical vapor deposition – CVD, plasma electrolytic oxidation – PEO and atmospheric plasma spraying – APS [4-7]. Atmospheric plasma spraying (APS) represents a proper technique for ceramic layers' deposition based on the high temperature of powders, high surface covered during deposition (robotic powder gun), industrial possibility of applications, high deposition rate and relative low price.

Contact Angle is an important parameter to measure surface wettability of solid surface. This technique implies to measure the angle formed by a liquid drop at the three-phase boundary where a liquid, gas, and solid meet. The *contact angle*, θ, is included between the tangent plane to the surface of the liquid and the tangent plane to the surface of the solid, at the point of intersection [8]. Low values for θ indicate that the interaction between liquid and solid are strong and the liquid tends to spread on the solid. High θ values indicate weak interaction and poor wetting [9]. If θ is less than 90°, then the liquid is said to wet (or sometimes partially wet) the solid. A zero-contact angle represents complete wetting. If θ is greater than 90°, then it is said to be non-wetting. A value 180° for θ indicate a super non-wettable solid surface [8]. Measurement of contact angles is recommended for a better knowledge of the interactions between ceramics and liquids, which play an important role in all applications that involve a contact environment.

Many medical and industrial applications of ceramic materials use alumina and zirconia as bulk or thin films [3] and the contact with a wet environment is frequently realized. Obtaining ceramic coatings from alumina and zirconia powders (combination in different wt%) satisfy many requirements like metallic base material properties in the same time with both involved ceramic characteristic coatings. Ceramic layer roughness plays an important role in the material properties influencing the microhardness, scratch behavior and droplet contact angle.

[1] GHEORGHE ASACHI TECHNICAL UNIVERSITY OF IASI, FACULTY OF MATERIALS SCIENCE AND ENGINEERING, PROF.DR.DOC. D. MANGERON NO. 41 STREET, 700050 IASI, ROMANIA
[2] GHEORGHE ASACHI TECH UNIV IASI, DEPT MACHINE MFG TECHNOL, 59A D MANGERON BLVD, IASI 700050, ROMANIA
[3] "GHEORGHE ASACHI" TECHNICAL UNIVERSITY OF IASI, DEPARTMENT OF PHYSICS, 700050 IASI, ROMANIA
[4] "GHEORGHE ASACHI" TECHNICAL UNIVERSITY OF IASI, DEPARTMENT OF SPORT, 700050 IASI, ROMANIA
[5] GHEORGHE ASACHI TECH UNIV IASI, FAC MECH ENGN 43 D MANGERON ST, IASI 700050, ROMANIA

* Corresponding author: nicanor.cimpoesu@tuiasi.ro

In this article insights about the growth of ceramic coatings through atmospheric plasma spraying using a robotic arm deposition system were given. After five passes homogeneous layers were obtained from a mixture of alumina and zirconia powders. Complex ceramic layers were analyzed before and after mechanical polish by structural point of view (SEM), roughness evolution (profilometer) and contact angle analysis.

2. Experimental details

2.1. Manufacturing of plasma spray ceramic layers

Ceramic layers were obtained from powders through APS using the parameters presented in TABLE 1. Powders were provided by Metco SC, an International producer of powders especially for Sulzer deposition gun used in this case to grow the ceramic layers. In this technique the powders reach extremely high temperatures between 12000-15000°C which melt entirely the ceramic oxides forming a homogeny mixture [4,5].

We perform 100 determinations of the powder's length, for Al_2O_3 and diameters for ZrO_2 powders using VegaTc software. Al_2O_3 powders have a rectangular shape, Fig. 1a), with micrometric dimensions: minimum value around 10 μm, maximum 60 μm and a mean value of 28 μm of width/length (Standard deviation was ±5 μm). Most of the ZrO_2 powders have a round shape, Fig. 1b), with an average diameter of 30 μm, a minimum size around 20 μm, a maximum value around 60 μm and an average circumference was of 100 μm. The shape of the powders used are, Fig. 1a) and b), for alumina mostly rectangular and for zirconia round.

In order to obtain layers with a proper continuity and homogeneity both shape and dimensions are important to combine two different types of powders. The mean values for both types of powders have close values (28 respectively 30 μm) encouraging the obtaining of homogeneous layers.

2.2. Surface analysis of APS ceramic layers

Ceramic particles, before and after mixture, and ceramic layers (before and after grinding) were investigated with scanning electron microscopy (SEM VegaTescan LMH II, SE detector, 30 kV electron gun power, 15.5 mm working distance

TABLE 1

Deposition parameters for Atmospheric Plasma Spraying (APS) of ceramic powders on metallic substrate. The parameters were choosing based on powders manufacturer recommendations

Powder	9 PM powders feeder			Gun	Distance Gun-target (mm)	Electric parameters		Ar		H_2	
	Carrier gas (NLPM)	Air pressure (MPa)	Quantity (g/min)			DC (A)	DC (V)	P (MPa)	Gas flow (NLPM)	P (MPa)	Gas flow (NLPM
Al_2O_3+ZrO_2	4.9	145	130	9PM	110	375	75-85	350	40	350	7

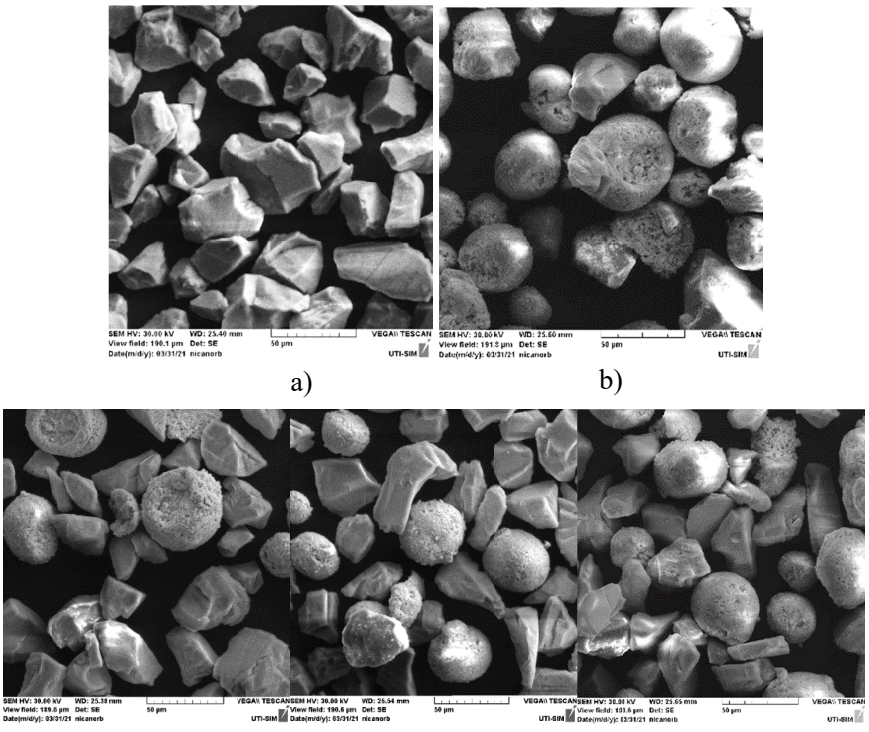

a) b) c) d) e)

Fig. 1. SEM images of Al_2O_3 and ZrO_2 powders: Al_2O_3 in a) ZrO_2, in b), Al_2O_3+25%ZrO_2 in c), Al_2O_3+50%ZrO_2 in d) and Al_2O_3+75%ZrO_2 in e)

from ESIM-Energy Spectroscopy and Microscopy Imaging Laboratory. A problem of the layers growth through APS are the cracks and pores from the surface [10]. The appearence of these is mainly atributed to the temperature difference between the deposited and partially chiled layer the the next one at highest temperature. In order to eliminate these structural elements that influence the ceramic layer properties a mechanical grinding was realized with metalographic papers till 2000 grid. Surface profile, before and after mechanical gringing, was determined on a Taylor Hobson FORM TALYSURF I50 equipment (sensitive peak made of conical diamond, investigation distance: 30 mm, Talymap-3D Analysis Programme Package). Five experiments were performed on each sample.

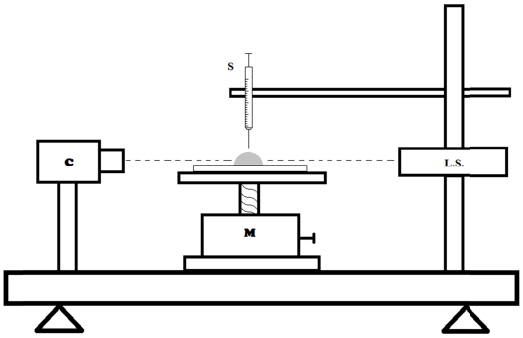

Fig. 2. Device used to measure the static contact angle

2.3. Contact angle analysis

In this paper, the static contact angle of a sessile drop placed on the solid surface was measured with sessile drop technique using the device from Fig. 2.

The equipment contains a video camera equipped with a suitable magnifying lens (C), a cold light source (L.S.), a sample stage whose elevation can be controlled to high precision (M), and a syringe (S) capable to deliver a droplet with a volume about 1 µl. The drop profile was photographed, and an image analysis software (Origin Pro 2021) was used to determine the tangent of the sessile drop profile at the three-phase contact point.

The contact angle measurements were made with three test liquids, namely water, ethanol, and glycerol. Ten different regions of the sample surface were selected, taking into consideration the contact angle values of three measurements. The thermodynamic equilibrium was established by waiting for a fixed time (10 s) before recording the contact angle, except for ethanol where the drops profiles were photographed as soon as were delivered to avoid spreading and evaporation.

3. Experimental results

3.1. Morphological analyze of ceramic coatings

In Fig. 3a)-c) are highlighted the aspects of the ceramic layers deposited through APC on carbon steel substrate. Formations of molten material are present on the surface with various shapes and orientations like droplets or pie splashes. General

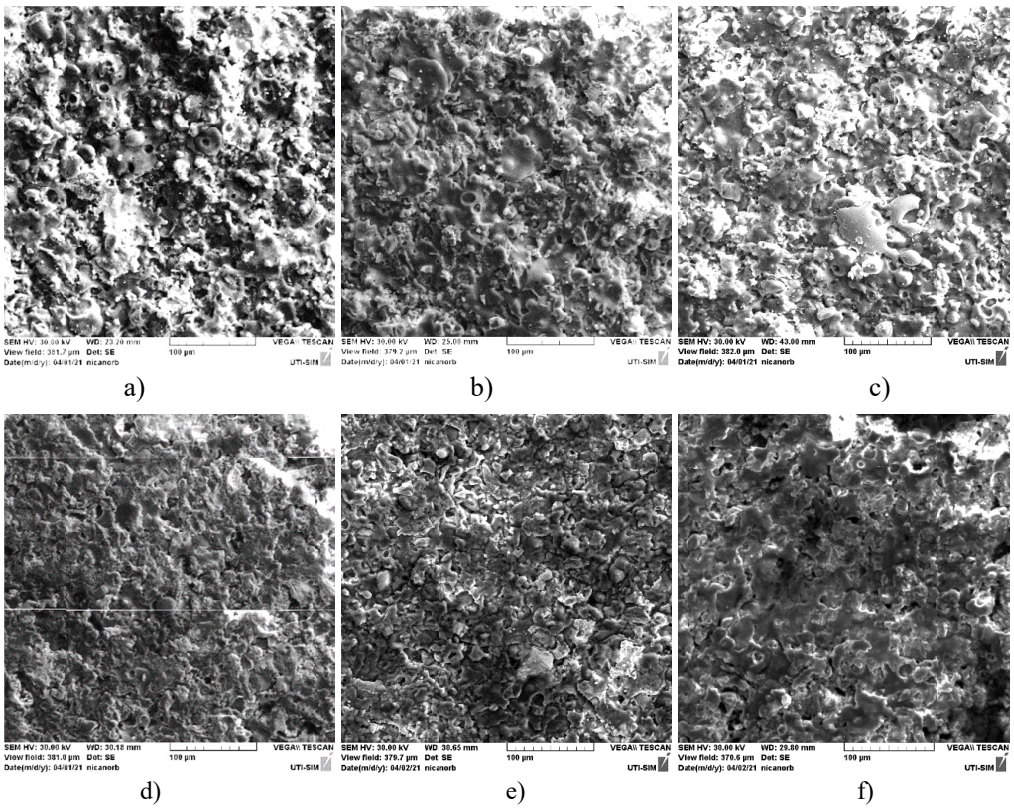

Fig. 3. SEM images of sample ceramic layers (a) Al_2O_3-25%ZrO_2, (b) Al_2O_3-50%ZrO_2 and (c) Al_2O_3-75%ZrO_2 and after mechanical grinding in d)-f)

aspects of the surface are of non-homogeneous structural material based on different shapes of the splashes. Increasing the zirconia percentage, Fig. 3c), more round shape elements appear on the surface. At macroscopic scale the surface is cracks free and only few pores are observed on the surface. At microscopic scale the presence of cracks is observed between same and especially different shape elements (alumina and zirconia).

After mechanical grinding of the ceramic layer surfaces, Fig. 3d)-f), the surface present, in all three cases, a more homogeneous aspect, a part of the big splashes was removed and we reveal the real microstructure of the mixture alumina-zirconia that we obtained through APS. Increasing the percentage of ZrO2, Fig. 3e) and f) a finer structure can be observed. The presence of pores and micro-cracks is also identified.

The roughness of the ceramic layer's surfaces varies consistent between initial state, Fig. 4a)-c) and mechanical grinded samples respectively Fig. 4d)-f). The main values obtained, TABLE 2, present the highest roughness on sample Al_2O_3-25%ZrO_2 with Ra (arithmetic mean roughness) = 3.67 µm that can be attributed to the higher percentage of alumina and their particle irregular shape. Before grinding the sample with 75%ZrO_2 present the most homogeneous surface by means of peaks and valleys presence. After grinding operation, all samples present a considerable decrease of the roughness, the smoother surface is of Al_2O_3-25%ZrO_2 sample probably because of the software nature of alumina. All samples, with or without mechanical grinding, present deep valleys which are pores characteristic for these types of coatings.

TABLE 2

Roughness parameters of the ceramic layer surfaces

Sample/ parameters	Substrate	P1	P1-p	P2	P2-p	P3	P3-p
R_a µm	—	3.67	0.34	2.78	0.43	2.60	0.61
R_q µm	—	3.93	0.46	3.55	0.58	3.27	0.96
R_{sk}	—	–0.13	–1.05	0.03	–0.22	–0.01	–1.95
R_{ku}	—	2.95	5.49	3.59	7.31	3.18	10.63
R_t µm	—	26.59	4.03	26.10	5.90	24.52	9.91
R_z µm	—	14.22	1.99	13.05	2.50	12.04	3.59

R_q (referred to as the root-mean-square roughness) present the smaller value in first sample case, after grinding, and the biggest value for the same sample before grinding. The zirconia percentage decrease the material R_q values in case of non-grinded material and increase these values in case of grinded materials.

Mean values of main characteristics on height direction of a surface profile are R_{sk} and R_{ku} (Skewness and Kurtosis). The dimension and sign of R_{sk} is given by the way the solid material is spread within the profile, in comparison to the median line, in our case, the material is more above the median line and then the value of the skewness parameter is negative. In one case P2 – TABLE 2, where the solid material is mainly below the median line then the value of the parameter R_{sk} is positive. Knowing that surface roughness were the heights have been removed, or with deep cracks, lead to negative values of the skewness parameter we can appreciate that the pores play an important role in determination of R_{sk} values in our case. After mechanical grinding

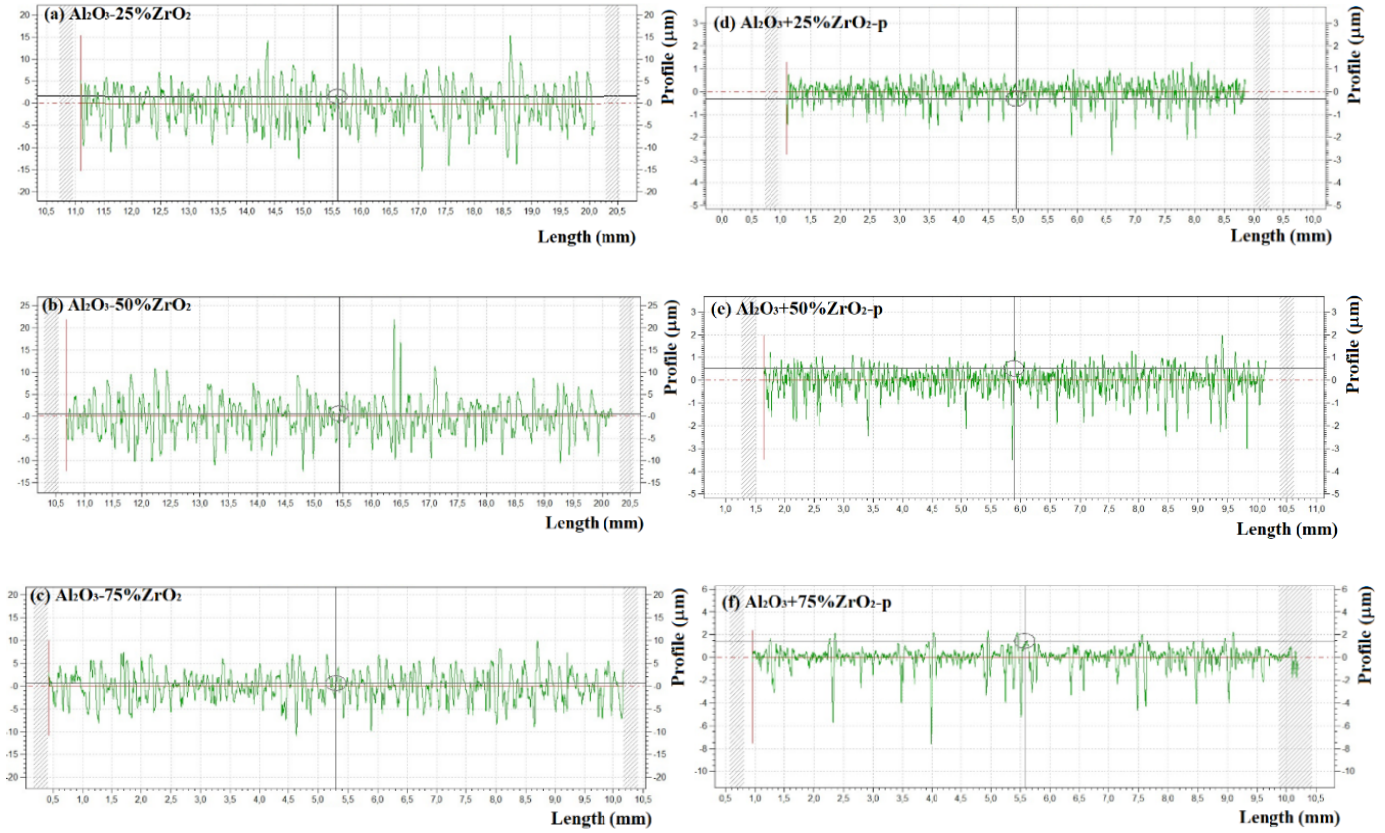

Fig. 4. Roughness profiles of samples after APS deposition: (a) Al_2O_3-25%ZrO_2, (b) Al_2O_3-50%ZrO_2 and (c) Al_2O_3-75%ZrO_2

most of the peaks were removed and values of R_{sk} increase also at negative part. In case of sample P2 the surface is formed by higher peaks, or smoother valleys having, before mechanical grinding a positive value of the R_{sk} parameter.

Another parameter that appreciates the form of a surface is the kurtosis parameter (R_{ku}). If a surface is characterized by many high tips and deep valleys, holes or pores then $R_{ku} > 3$ (a leptokurtic profile) while if compared with the median line the surface present a reduced number of heights or valleys, a platykurtic profile results – $R_{ku} < 3$. Excepting sample P1 with 2.95 all the other samples present a R_{ku} parameter bigger than 3 and for grinded samples even bigger than 5,7 respectively 10. R_t (total height of surface is the vertical distance between the maximum profile peak height and the maximum profile valley depth along the evaluation length) parameter present similar values before grinding and differences after polishing based on the samples micro-hardness of the surface [11-13].

The maximum height of the profile (R_z – indicates the absolute distance between the maximum profile peak height and the maximum profile valley depth along the profile length) presents the highest and smallest values on the same sample respectively P1 before (14.22 μm) and after (1.99 μm) mechanical grinding showing that the softer sample as surface hardness is P1. All samples in grinded state present an important reduction of R_z values through substantial reduction of peaks during mechanical polish.

Measurement of Static Contact Angles

Based on Fowkes surface energy theory, which combine the Young and Young-Dupree equations [14,15], the values of the contact angles, measured with the three test liquids were used to determine the surface polarity. In this method, the surface energy has two components: a dispersive and a polar one. The dispersive component is used to evaluate the work of adhesion, expressed as, Eq. (1):

$$W_a = 2\sqrt{\gamma_l^{\,d} \cdot \gamma_s^{\,d}} + 2\sqrt{\gamma_l^{\,p} \cdot \gamma_s^{\,p}} = \gamma_l \left(1 + \cos\theta\right) \qquad (1)$$

In this equation, θ is the contact angle of a test liquid. The indices l and s are states of the test liquid and the polymer solid sample, while the indices d and p are associated with the disperse and polar components of the surface tension.

To determine the surface tension of the solid surface, the surface tension components of the test liquids were taken from the literature [16] and Eq. (2) was applied.

$$\gamma_s = \gamma_s^{\,d} + \gamma_s^{\,p} \qquad (2)$$

The surface polarity was then evaluated using Eq. (3):

$$P = \frac{\gamma_s^{\,p}}{\gamma_s} = \frac{\gamma_s^{\,p}}{\gamma_s^{\,d} + \gamma_s^{\,p}} \qquad (3)$$

The polar and dispersive surface energy components of the tree test liquids used in this study: water (W), ethanol (E), and glycerol (G) are listed in TABLE 3.

TABLE 3

Polar and dispersive surface energy components of the test liquid

Test Liquid	γ_1 (mJ/m^2)	$\gamma_1^{\,p}$ (mJ/m^2)	$\gamma_1^{\,d}$ (mJ/m^2)
Water (W)	72.8	51.0	21.8
Ethanol (E)	22.4	18.8	3.6
Glycerol (G)	64	30	34

To analyze the surface properties, the values of ethanol and glycerol contact angles, from TABLE 4, were introduced in Eq. (1). The values obtained are displayed in TABLE 5.

TABLE 4

The contact angles of water, glycerol, and ethanol for samples with different percent of ZrO_2 and Al_2O_3 deposited on steel substrate, before and after polishing process of the samples

Sample		Contact Angle (degree)		
	Percent of ZrO_2 and Al_2O_3 deposited on substrate	Water (W)	Ethanol (E)	Glycerol (G)
Before polishing process	P1 (ZrO_2-25%+Al_2O_3-75%)	96.54	3.44	94.68
	P2 (ZrO_2-50%+Al_2O_3-50%)	108.61	5.44	118.69
	P3 (ZrO_2-75%+Al_2O_3-25%)	113.55	4.87	114.31
After polishing process	P1 (ZrO_2-25%+Al_2O_3-75%)	99.92	14.11	104.20
	P2 (ZrO_2-50%+Al_2O_3-50%)	51.76	17.45	84.65
	P3 (ZrO_2-75%+Al_2O_3-25%)	102.89	13.21	104.22
Steel substrate		37.60	13.18	49.79

For all samples, obtained before and after polishing process, the dispersive component of surface tension is higher than its polar one, except for the steel substrate.

TABLE 5

The surface tension components of samples with different percent of ZrO_2 and Al_2O_3 deposited on steel substrate, before and after polishing process of the samples

Sample	Percent of ZrO_2 and Al_2O_3 deposited on substrate	$\gamma_s^{\,p}$ (mN/m)	$\gamma_s^{\,d}$ (mN/m)	γ_s (mN/m)	P (%)
Before polishing process	P1 (ZrO_2-25%+Al_2O_3-75%)	1.16	30.90	32.05	3.60
	P2 (ZrO_2-50%+Al_2O_3-50%)	4.60	16.88	21.48	21.41
	P3 (ZrO_2-75%+Al_2O_3-25%)	1.03	30.15	31.17	3.29
After polishing process	P1 (ZrO_2-25%+Al_2O_3-75%)	0.11	25.16	25.27	0.44
	P2 (ZrO_2-50%+Al_2O_3-50%)	11.34	43.93	55.27	20.52
	P3 (ZrO_2-75%+Al_2O_3-25%)	7.48	40.37	47.84	15.63
Steel substrate		51.92	3.78	55.71	93.21

Polar components increase for 25% and 50% percent of ZrO_2 and decrease when 75% of ZrO_2 was deposited.

The surface free energy of hydration, ΔG_w, was estimated to evidence the effects of ZrO_2 deposited on the steel substrate.

The critical value for ΔG_w is –113 mJ/m. It represents the equilibrium between hydrophilicity and hydrophobicity of the studied surface. For $\Delta G_w < -113$ mJ/m, the examined surface can be considered hydrophilic, while, when $\Delta G_w > -113$ mJ/m, it should be considered hydrophobic [17,18].

Eq. (4) [14] was used for the determination of ΔG_w. The contact angles of water, θ_w for the samples with different percent of ZrO_2 and Al_2O_3 deposited on steel substrate, before and after polishing process of the samples were from TABLE 2, and the total surface tension of water, γ_l, was 72.8 mN/m [16].

$$\Delta G_w = -\gamma_l(1 + \cos\theta_w) \quad (4)$$

The dependence of the surface free energy of hydration on the percent of ZrO_2 deposited on the steel substrate is evidenced in figure 5 for the samples before and after the polishing process.

From Fig. 2 it results that the steel substrate is hydrophilic and become hydrophobic when ceramic layer was deposited. Surface free energy of hydration increases for all the samples with addition of zirconia before polishing process. One can observe that ΔG_w reached the limit between hydrophilicity and hydrophobicity for the sample which contains 50% ZrO_2 and 50% Al_2O_3 after the polishing process.

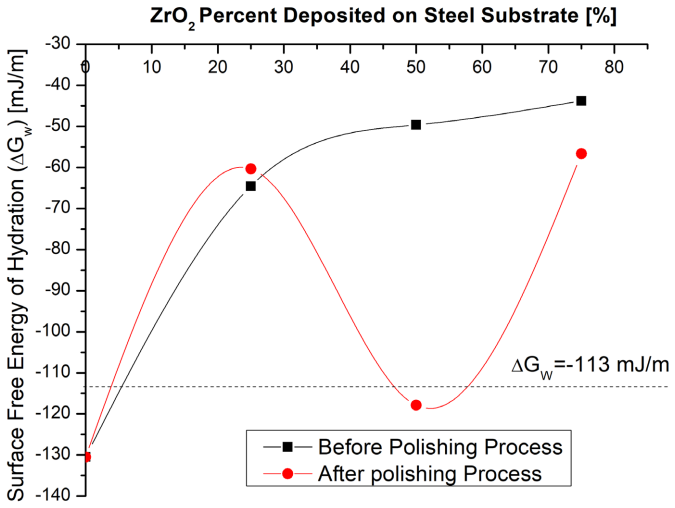

Fig. 5. The dependence of the surface free energy of hydration on the percent of ZrO_2 deposited on the steel substrate before and after the polishing process

Conclusions

Ceramic complex coatings (alumina-(25, 50 and 75%) zirconia) were obtained using an atmospheric plasma spraying system on metallic substrate. Structural analyze performed on the surface of the layers present a fairly structural homogenization of the coatings, a high decrease of the roughness with mechanical grinding and the presence of micro-cracks and pores on the structure.

Steel substrate surface is hydrophilic and become hydrophobic when ceramic layer was deposited. Surface free energy of hydration increases for all the coatings with addition of zirconia before polishing process. One can observe that surface free energy of hydration is situated at the boundary between hydrophilicity and hydrophobicity for the sample which contains 50% ZrO_2 and 50% Al_2O_3 after the polishing process.

Acknowledgments

This work was supported by a grant of the Romanian Ministry of Education and Research, CNCS – UEFISCDI, project number PN-III-P1-1.1-TE-2019-1921, within PNCDI III.

REFERENCES

[1] S.M. Dezfuli, M. Sabzi. Deposition of ceramic nanocomposite coatings by electroplating process: A review of layer-deposition mechanisms and effective parameters on the formation of the coating. Ceram. Int. **45**, 21835-21842 (2019). DOI: https://doi.org/10.1016/j.ceramint.2019.07.190

[2 Q. Chang, L. Zhang, X. Liu, D. Peng, G. Meng, Preparation of crack-free ZrO_2 membrane on Al_2O_3 support with ZrO_2-Al_2O_3 composite intermediate layers, J. Membrane Sci. **250**, 105-111 (2005). DOI: https://doi.org/10.1016/j.memsci.2004.10.020

[3] S. Sathish, M. Geetha, Comparative study on corrosion behavior of plasma sprayed Al2O3, ZrO2, Al2O3/ZrO2 and ZrO2/Al2O3 coatings, Trans. Nonferrous Met. Soc. China **26** 1336-1344 (2016). DOI: https://doi.org/10.1016/S1003-6326(16)64236-X

[4] C. Florea, C. Bejinariu. C. Munteanu, N. Cimpoesu, Preliminary Results on Complex Ceramic Layers Deposition by Atmospheric Plasma Spraying, Advanced Materials Engineering and Technology V, Book Series: AIP Conference Proceedings **1835**, UNSP 020053 (2017). DOI: https://doi.org/10.1063/1.4983793

[5] C.D. Florea, C. Munteanu, N. Cimpoesu, I.G. Sandu, C. Baciu, C. Bejinariu, Characterization of Advanced Ceramic Materials Thin Films Deposited on Fe-C Substrate, Rev. de Chimie **68**, 11 (2017).

[6] B. Istrate, J.V. Rau, C. Munteanu, I.V. Antoniac, V. Saceleanu, Properties and in vitro assessment of ZrO2-based coatings obtained by atmospheric plasma jet spraying on biodegradable Mg-Ca and Mg-Ca-Zr alloys, Ceram. Int. Part: B **46**, 15897-15906 (2020). DOI: https://doi.org/10.1016/j.ceramint.2020.03.138

[7] C.C. Paleu, C. Munteanu, B. Istrate, S. Bhaumik, P. Vizureanu, M.S. Baltatu, V. Paleu, Microstructural Analysis and Tribological Behavior of AMDRY 1371 (Mo-NiCrFeBSiC) Atmospheric Plasma Spray Deposited Thin Coatings, Coatings, **10** 1186 (2020). DOI: https://doi.org/10.3390/coatings10121186.

[8] H.Y. Erbil, Surface Chemistry of Solid and Liquid Interfaces, Blackwell Publishing Ltd (2006), ISBN-10: 1-4051-1968-3.

[9] C.J. Van Oss, Interfacial Forces in Aqueous Media; Marcel Dekker Inc.: New York, NY, USA (1994).

[10] M.S. Baltatu, P. Vizureanu, A.V. Sandu, C. Munteanu, B. Istrate, Microstructural analysis and tribological behavior of Ti-based alloys with a ceramic layer using the thermal spray method, Coatings **10**, 1216 (2020). DOI: https://doi.org/10.3390/coatings10121216

[11] M. Benchea, S. Cretu, Surface roughness influence on active surfaces geometry and modified rating life of rolling contacts, IOP Conference Series-Materials Science and Engineering **724**, 012025 (2020). DOI: https://doi.org/10.1088/1757-899X/724/1/012025

[12] I. Oancea, C. Bujoreanu, M. Budescu, M. Benchea, C.M. Gradinaru, Considerations on sound absorption coefficient of sustainable concrete with different waste replacements, J. Clean. Prod. **203**, 301-312 (2018).
DOI: https://doi.org/10.1016/j.jclepro. 2018.08.273, 2018.

[13] C. Bujoreanu, S. Irimiciuc, M. Benchea, A fractal approach of the sound absorption behaviour of materials. Theoretical and experimental aspects, Int. J. Nonlin. Mech. **103**, 127-137 (2018). DOI: https://doi.org/10.1016/j.ijnonlinmec.2018.05.005

[14] D.H. Kaelble, Dispersion-polar surface tension properties of organic solids. J. Adhes **2**, 66-81 (1970).

[15] A.V. Sandu, M.S. Baltatu, M. Nabialek, A. Savin, P. Vizureanu, Characterization and Mechanical Proprieties of New TiMo Alloys Used for Medical Applications, Materials 12 (18), 2973 (2019). DOI: https://doi.org/10.3390/ma12182973

[16] M. Rankl, S. Laib, S. Seeger, Surface tension properties of surface-coatings for application in biodiagnostics determined by contact angle measurements. Coll. Surf. B. Biointerf. **30**, 177-186 (2003). DOI: https://doi.org/10.1016/S0927-7765(03)00085-7

[17] R.S. Faibish, W. Yoshida, Y. Cohen,. Contact Angle Study on Polymer-Grafted Silicon Wafers. J. Coll. Interf. Sci. **256**, 341-350 (2002). DOI: https://doi.org/10.1006/jcis.2002.8612

[18] A. Tandjaoui, M. Cherif, L. Carroz, J. Sanchez, R. Reboud, C. Garnier, T. Duffar, Investigation of liquid oxide interactions with refractory substrates via sessile drop method, J. Mater. Sci. **51**, 1701-1712 (2016).
DOI: https://doi.org/10.1007/s10853-015-9504-0